Available online at www.sciencedirect.com
SCIENCE DIRECT®
Acta Materialia 52 (2004) 4537–4545
Acta MATERIALIA
www.actamat-journals.com

Grain boundary wetting by a solid phase; microstructural development in a Zn–5 wt% Al alloy

G.A. López [a,*], E.J. Mittemeijer [a], B.B. Straumal [b]

[a] *Max Planck Institute for Metals Research, Heisenbergstr. 3, D-70569 Stuttgart, Germany*
[b] *Institute of Solid State Physics, Russian Academy of Sciences, Chernogolovka, 142432 Moscow, Russia*

Received 19 April 2004; received in revised form 26 May 2004; accepted 8 June 2004
Available online 2 July 2004

Abstract

A systematic study of grain boundary wetting by a solid phase was carried out for the first time. The microstructure of Zn–5 wt% Al polycrystals was studied in the temperature range 250–375 °C. The Al-rich phase formed either chains of separated lens-like precipitates or continuous layers at the Zn-rich phase/Zn-rich phase grain boundaries upon annealing at different temperatures. The contact angle at the intersection between the Al-rich phase/Zn-rich phase interphase boundaries and the Zn-rich phase/Zn-rich phase grain boundary decreased with increasing temperature. It became zero at a certain temperature, and remained zero above this *solid-state wetting temperature*, i.e., a continuous Al-rich phase layer covered the Zn-rich phase/Zn-rich phase grain boundaries. The fraction of wetted grain boundaries increased with increasing temperature and was independent of annealing time. The growth of the Al-rich phase at the grain boundaries is controlled by volume diffusion in the matrix phase.

Keywords: Grain boundaries; Wetting; Phase diagrams; Zn–Al alloys

1. Introduction

Decomposition of supersaturated solid solutions is a very important process occurring upon heat treatment of materials, because thereby the microstructure of the alloy can be changed and thus the properties of the material can be controlled.

Precipitation at grain boundaries can occur easier than in the bulk, because the reduction of grain-boundary area and thus grain-boundary energy favours nucleation [1]. Two morphologies may be distinguished for second-phase (β) particles at a grain boundary (GB) in the matrix (α):

(1) If the GB energy of grains in the matrix α per unit area, $\sigma_{GB}^{\alpha\alpha}$, is smaller than two times the energy per unit area of the α/β interphase boundary (IB), $\sigma_{IB}^{\alpha\beta}$, formed upon precipitation of the β particle on the α/α GB, then the growing β particle tends to reduce its surface, and develops a lens-like shape characterized by a contact angle θ (see Fig. 1(d)). If the surface tensions at the junction of the GB and the IBs are balanced (in "equilibrium"), it holds $\sigma_{GB}^{\alpha\alpha} = 2\sigma_{IB}^{\alpha\beta}\cos(\theta/2)$ [2]. This equation holds for isotropic interfacial energies and for a stress-free state.
(2) If $\sigma_{GB}^{\alpha\alpha} > 2\sigma_{IB}^{\alpha\beta}$, the growing β particle tends to increase its surface: a layer of β-phase covers continuously ("wets") the α/α GB (Fig. 1(e)). In other words: the α/α GB is unstable in contact with the growing β particle and the "equilibrium" (see above) contact angle θ is nil.

Layers of solid second phases fully covering the GBs in a matrix have been observed in many systems. Important examples are Fe_3C layers at GBs in ferritic and austenitic steels [3,4], layers of Cu at GBs in sintered W polycrystals [5–8], α-Zr layers at GBs of β-(Zr, Nb) [9]

* Corresponding author. Tel.: +49-711-689-3318; fax: +49-711-689-3312.
E-mail address: g.a.lopez@mf.mpg.de (G.A. López).

1359-6454/$30.00 © 2004 Acta Materialia Inc. Published by Elsevier Ltd. All rights reserved.
doi:10.1016/j.actamat.2004.06.011

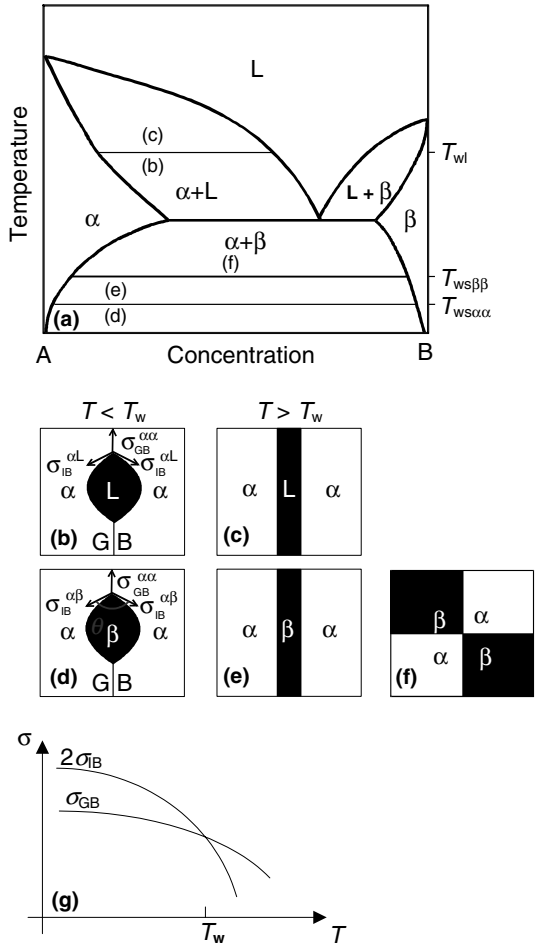

Fig. 1. (a) Schematic phase diagram showing tie-lines of GB wetting by a liquid phase and of GB wetting by a solid phase at T_{wl}, and $T_{ws\alpha\alpha}$ and $T_{ws\beta\beta}$, respectively. (b) Liquid phase L does not wet a GB in the solid phase α ($T < T_{wl}$). (c) Liquid phase L wets a GB in the solid phase α ($T > T_{wl}$). (d) Solid phase β does not wet a GB in the solid phase α ($T < T_{ws\alpha\alpha}$). (e) Solid phase β wets a GB in the solid phase α ($T > T_{ws\alpha\alpha}$). (f) Only α/β IBs exist in an α + β polycrystal if wetting occurs at both α/α and β/β GBs ($T > T_{ws\beta\beta}$). (g) Schematic dependencies of σ_{GB} and $2\sigma_{IB}$ on temperature. The point of intersection indicates the wetting temperature, T_w.

and Bi layers at GBs in Cu [10]. Such continuous GB layers of a solid second phase can have either detrimental effects (e.g. enhanced brittleness) or favourable effects (e.g. improved plasticity).

The GB wetting (covering) by a layer of a *solid* second phase is analogous to the conventional GB wetting by a *liquid* second phase [11–18]: cf. Fig. 1(b)–(e). The value of the temperature is decisive for the occurrence of wetting. With increasing temperature both the GB energy $\sigma_{GB}(T)$ and the IB energy $\sigma_{IB}(T)$ decrease normally. If, at sufficiently low temperature $2\sigma_{IB} > \sigma_{GB}$ and, upon increasing temperature, the temperature dependencies $\sigma_{GB}(T)$ and $2\sigma_{IB}(T)$ intersect (Fig. 1(g)), then a GB wetting proceeds at the temperature T_w of intersection and at temperatures higher than T_w (cf. points (1) and (2)). Starting from a relatively low temperature, upon increasing the temperature the contact angle θ decreases down to $\theta = 0$ at T_w. Above T_w the contact angle remains $\theta = 0$ (Fig. 1(c) and (e)). The *tie-line of GB wetting*, i.e. the tie-line connecting the phases in equilibrium at T_w, can be drawn in the two-phase regions (α + L) and (α + β) of the phase diagram for the cases of liquid and solid GB wetting (Fig. 1(a)). At and above this tie-line the second, *liquid* or *solid*, phase forms a layer separating the crystals. GBs with a relatively low energy possess a relatively high T_w. In polycrystalline materials a spectrum of GBs with different energies exists. Therefore, in polycrystals a range of T_w values occurs: from T_{wmin} to T_{wmax}. Corresponding tie-lines at T_{wmin} and T_{wmax} for wetting by a liquid phase have been presented in the Al–Sn, Al–Mg and Al–Zn phase diagrams [15,17,18]. Above T_{wmax} all GBs are completely wetted. At temperatures between T_{wmin} and T_{wmax} only a fraction of the total number of GBs is wetted. Below T_{wmin} all GBs are not wetted, and the second phase appears at the GBs only as (chains of) isolated particles. Peculiar electrical and mechanical properties of materials can be caused by a layer of a second phase fully covering the GBs. This has relevance especially for nanocrystalline materials that have a large volume fraction of GBs. Tie-lines as mentioned can then be very useful with a view to practical applications.

The "wetting" phenomenon, although described above deliberately in a general way, has until now been discussed and observed in the literature with respect to wetting by a *liquid* phase. The purpose of this contribution is to demonstrate that "wetting" by a solid phase can occur and be explained on the basis of the same thermodynamic background. The following predictions can thus be made in advance:

- *Transition* from incomplete coverage (wetting) of a single GB by a solid second phase to complete coverage (wetting) of that GB with increasing temperature at a certain, solid-state wetting temperature, T_{ws}.
- Dependence of T_{ws} on the GB energy (low T_{ws} for high $\sigma_{GB}^{\alpha\alpha}$ and vice versa).
- Increase of the fraction of GBs covered by a solid phase from 0 to 100% with increasing temperature from T_{wsmin} to T_{wsmax}.

These phenomena of solid-phase wetting have been studied and discussed for the first time in this work. To this end the Al–Zn system has been chosen. For this system the occurrence of conventional liquid-phase wetting was shown recently for the two-phase ((Al) + L) region of the Al–Zn phase diagram [18]. The current study demonstrates the occurrence of solid-phase wetting and, as a final result, provides the tie-line for first occurrence of solid-phase wetting in the Al–Zn phase diagram.

2. Experimental details

A Zn–5 wt% Al alloy was produced by melting the corresponding amounts of Zn (99.999 wt%, Hereaus) and Al (99.9995 wt%, VAW Aluminium AG), and subsequent cooling down under vacuum (residual pressure of about 10^{-5} Pa). Slices (2 mm thick) of the alloy were prepared by sawing, grinding and chemical etching for 15 s (using a 5 wt% HF aqueous solution). Next, these samples were sealed in evacuated silica ampoules (residual pressure of approximately 10^{-4} Pa) and annealed in a tube furnace at several temperatures between 250 and 375 °C (see Fig. 2) for 336, 672 and 2016 h (temperature control within 1 °C). Thereafter, the specimens were quenched by crushing the ampoules in water.

The microstructure of the specimens was studied by optical microscopy (microscope Zeiss Axiophot) and scanning electron microscopy (field emission microscope JEOL JSM 6300 F). For the metallographic investigations, the samples were etched for 15 s with a 5 wt% HF aqueous solution.

The quantification of the wetted GBs by light microscopical analysis was performed adopting the following criterion: every GB was considered to be wetted only when a continuous layer had covered the whole (visible part of the) GB; if such a layer appeared to be interrupted, the GB was regarded as a non-wetted GB. At least 100 GBs were analysed at each temperature. In addition, using an imaging software (ProImage 3.20) the thicknesses of the second phase at the GBs were measured to investigate the growth kinetics. The average thickness value from 40 to 50 measurements and the corresponding standard deviation were determined for every annealing time (see above) at 250, 275, 283, 345 and 375 °C. The accuracy of these kinetic data would be enhanced by applying longer annealing times at the temperatures mentioned, but the relative slowness of the process makes this impossible for a practical period of time of investigation (longest annealing time applied was 2016 h).

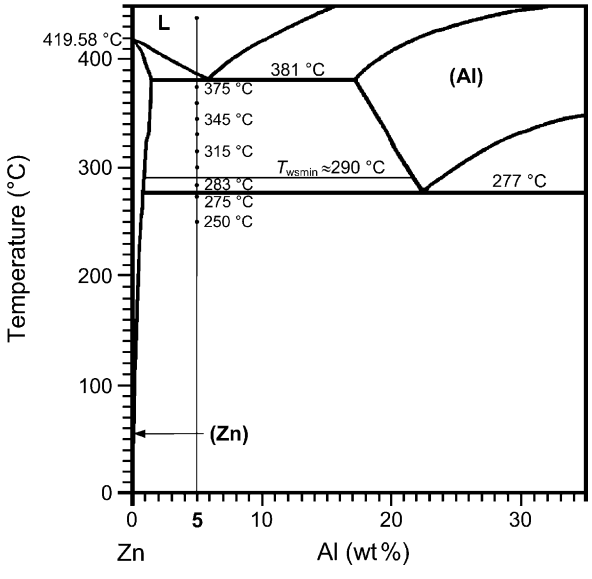

Fig. 2. The Zn–Al equilibrium phase diagram [19]. The vertical thin line represents the Zn–5 wt% Al alloy of this study. Points at that line represent the annealing temperatures applied. The tie-line at $T_{wsmin} \approx 290$ °C represents the minimal temperature determined in this work for wetting of Zn-rich phase/Zn-rich phase GBs by the Al-rich phase.

To confirm the presence of the different phases X-ray diffraction (XRD) patterns were taken from cross-sections of the samples. The XRD data were recorded employing a Philips X'Pert MPD diffractometer equipped with a graphite monochromator applying Co Kα radiation. The data were acquired in the diffraction angle range 20–120°, with a step width of 0.05° and a step time of 25 s. To identify the phases the characteristic peaks were compared with those given in the database of the International Centre for Diffraction Data (see cards 89–4037 for Al and 87–0713 for Zn). In addition, the reflection positions were determined by peak fitting with symmetric pseudo-Voigt functions (PROF-IT; Sonneveld & Delhez, 1996). From these data the lattice parameters were determined for both phases.

The measurement of the chemical composition of the phases was carried out using electron probe microanalysis (EPMA; Cameca SX100 instrument equipped with five wavelength-dispersive spectrometers). The measurements were performed at an accelerating voltage of 15 kV, a beam current of 20 nA and a take-off angle of 40°. The time per single point measurement was 60 s. The intensities of the Kα X-ray lines were taken as the difference between the peak maxima and the background intensities at the left and right sides of the peaks using thallium–acid–phthalate (for Al) and large-area LiF (for Zn) crystals as monochromators. The measured Al Kα and Zn Kα intensities were divided by those of pure Al and Zn standards, respectively. Then the composition was calculated from the corresponding intensity ratios applying the approach described in Ref. [20]. For the determination of the concentration profiles the electron beam was moved along a straight line on the specimen cross-sections with intervals from 1 to 5 μm between the locations for point measurements.

3. Results and discussion

3.1. As-cast microstructure

The as-cast microstructure of the as-prepared Zn–5 wt% Al alloy, i.e. after solidification and cooling down to room temperature, is shown in Fig. 3. Eutectic colonies of Al-rich phase and Zn-rich phase lamellae, formed at the eutectic temperature $T_e = 381$ °C during

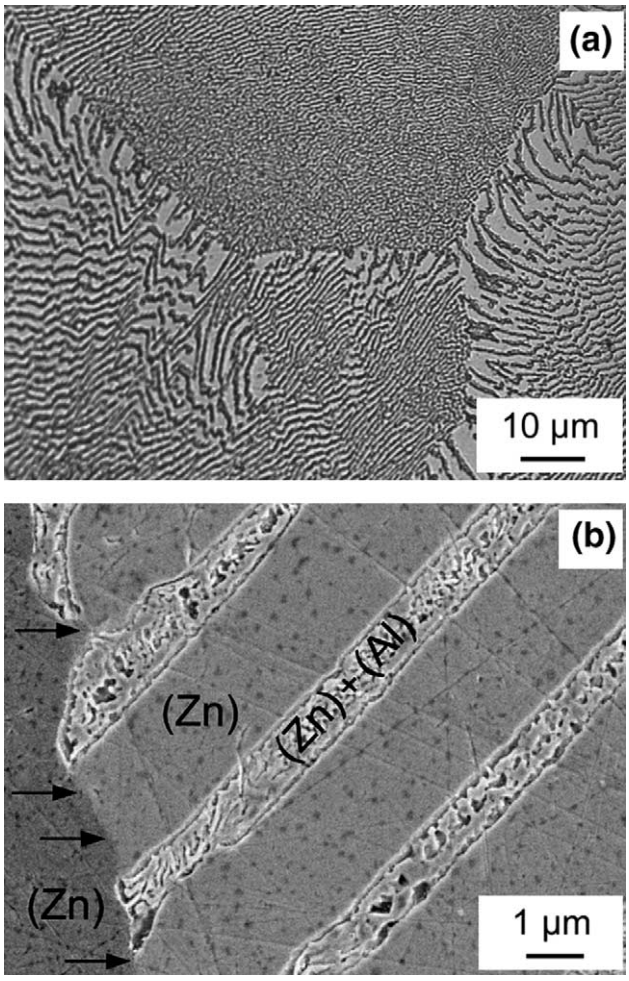

Fig. 3. Optical (a) and secondary-electron (b) micrographs of cross-sections of the as-cast Zn–5 wt% Al alloy after cooling down to room temperature. A Zn-rich phase/Zn-rich phase GB is marked by arrows (b).

solidification, can be observed clearly (Fig. 3(a); see Fig. 2 for the Zn-rich part of the Al–Zn phase diagram). EPMA indicates the existence of (only) two phases in these alloys, namely, the Al-rich and Zn-rich solid solutions. In the optical micrographs, the Zn-rich phase appears with a light grey colour and the Al-rich phase appears with a dark grey colour (Fig. 3(a)). Since the composition of the studied alloy is very close to the eutectic one, almost no primary Zn-rich phase crystals are present in the samples. The volume fraction of the Zn-rich phase solid solution in the eutectic is much larger than that of the Al-rich solid solution, in accordance with the lever rule. Therefore, each eutectic colony can be conceived as a Zn-rich grain containing Al-rich lamellae, and thus neighbouring eutectic colonies are separated by Zn-rich phase/Zn-rich phase GBs. Practically, no Al-rich phase/Al-rich phase GBs occurred as colony boundaries; the Al-rich lamellae of neighbouring eutectic colonies meet at the Zn-rich phase/Zn-rich phase GBs as two combs.

Upon casting, during the cooling to room temperature, a second (monotectoid) transformation proceeds at $T_{mt} = 277$ °C in the Al-rich lamellae: the Al-rich solid solution with an Al content in the range of about 17–22 wt% (cf. the phase diagram; Fig. 2) decomposes into an Al-richer solid solution (containing more than 67.6 wt% Al [19]) and the Zn-rich solid solution. The corresponding, resulting fine structure of the parent eutectic Al-rich phase lamellae can be seen in Fig. 3(b) (see also Figs. 4(c) and 5(a)).

3.2. Morphology of the grain-boundary precipitation

Long-time annealings of the as-cast specimens at several temperatures between 250 and 375 °C led to drastic changes of the initial microstructure. Typical microstructures of Zn–5 wt% Al alloys annealed at 250, 283, 345 and 375 °C are shown in Fig. 4. In all samples coarsening of the Al-rich phase lamellae had occurred in the bulk and Al-rich phase precipitates had grown at the Zn-rich phase/Zn-rich phase GBs. Note that after casting no precipitates were observed at the Zn-rich phase/Zn-rich phase GBs (see Fig. 3(a) and (b)). In Fig. 3(b) the Al-rich lamellae of the (former) eutectic microstructure are indicated as (Zn) + (Al). These solid solutions, (Zn) + (Al), formed by the monotectoid reaction at $T \leqslant 277$ °C, are nearly pure Zn and pure Al, respectively, according to the phase diagram (Fig. 2). Upon heating of the as-cast specimens from room temperature to the annealing temperature, the Al-rich lamellae ((Zn) + (Al)) become a single Al-rich phase (again) after crossing the monotectoid temperature ($T_{mt} = 277$ °C). The amount and composition of this Al-rich phase in the specimen may be approximately given by the equilibrium values at a temperature slightly above the temperature of the monotectoid reaction experienced during the preceding solidification (cf. Fig. 2 and Section 3.1 and results given in Section 3.3). Then, the (subsequent) annealing at $T_{mt} < T < T_e$ involves that the existing Al-rich phase has to adjust its composition by dissolution of Al in the surrounding Zn-rich phase and that new, additional Al-rich phase has to be formed, as follows from the phase diagram (Fig. 2). Against this background the development of Al-rich phase at the Zn-rich phase/Zn-rich phase GBs can then be understood as driven by a favourable change in the (total) interface energy (cf. Section 2). Indeed, adjacent to the precipitates at Zn-rich phase/Zn-rich phase GBs a depleted, precipitate-free zone can be observed (Fig. 4(a)–(d)).

Two different kinds of morphologies have been observed for the precipitates at the Zn-rich phase/Zn-rich phase GBs, depending on the annealing temperature. Chains of more or less isolated precipitates are observed at GBs of a specimen annealed at the relatively low temperature of 250 °C for 672 h (Fig. 4(a)). A continuous solid Al-rich phase layer covering certain GBs is

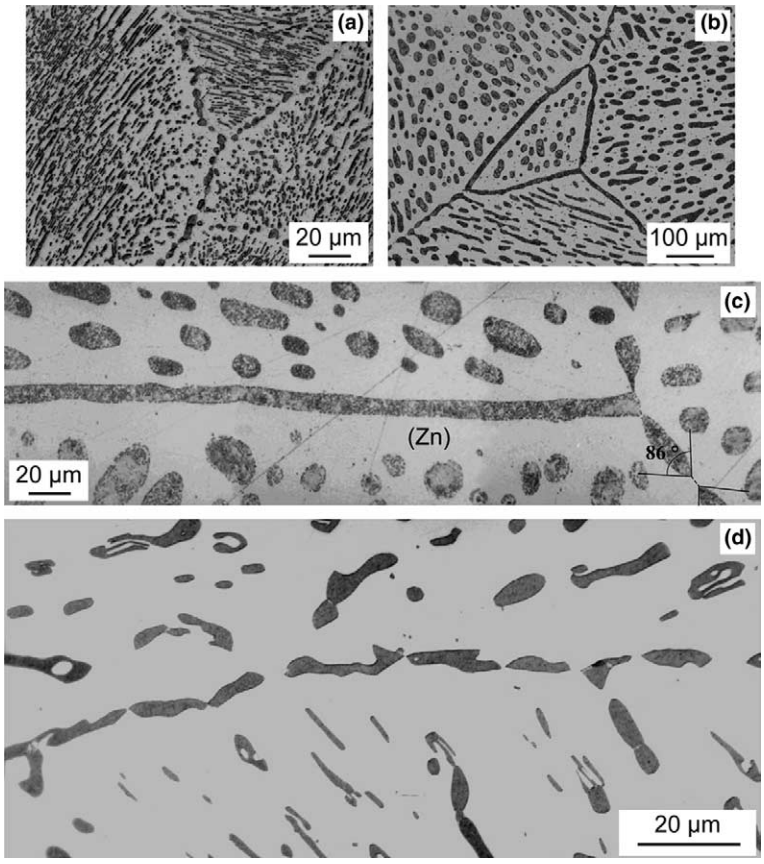

Fig. 4. Optical micrographs of the cross-sections of samples annealed for 672 h at 250 °C (a), 375 °C (b) and 345 °C (c), and annealed for 2016 h at 283 °C (d).

observed in specimens annealed at relatively high temperatures (Fig. 4(b)).

A triple junction of Zn-rich phase/Zn-rich phase GBs is shown in Fig. 4(c). The GB positioned horizontally is fully covered by a uniform Al-rich phase layer. The two GBs on the right-hand side of the micrograph are covered by chains of lens-like Al-rich phase precipitates. The contact angle θ for the precipitate particle and the GB of the latter type at the triple junction is about 86° (Fig. 4(c); cf. Fig. 1(d)).

The temperature of annealing appears to be decisive if wetting can occur: even 2016 h of annealing at the relatively low temperature of 283 °C did not lead to "wetted" GBs (Fig. 4(d)). To verify that the observations on solid-phase grain-boundary wetting do not depend on the pre-history of the specimen, specimens annealed at 250, 275 and 283 °C were annealed additionally at 375 °C. Note that after the anneals at 250, 275 and 283 °C no covered GBs occurred (see Section 3.4 and Fig. 6). After the additional anneal at 375 °C for two days covered GBs appeared indeed: the microstructure was the same as that shown in Fig. 4(b). Also the fraction of covered GBs, determined as about 35%, well agrees with the value obtained after annealing of as-cast samples directly at 375 °C (Fig. 6). Hence, the temperature appears to be a state variable for grain-boundary wetting by a solid phase.

As expected, with increasing annealing time at constant temperature all kinds of Al-rich phase precipitates coarsen. The coarsening is more pronounced at higher temperatures (Fig. 4(a) and (b)). The Al-rich phase lamellae in the bulk become unstable, break up and start to spheroidize. If individual precipitates occur at the GBs, upon continued annealing at the same temperature they remain lens-like. The continuous Al-rich phase layers at the GBs thicken with increasing annealing time.

It can be concluded that GB wetting by a solid phase proceeds in the two-phase (Zn-rich phase + Al-rich phase) area of the Al–Zn bulk phase diagram confined by the eutectic and monotectoid temperatures, if the temperature is above a critical value.

3.3. Composition of the Al-rich and Zn-rich phases

The composition of the phases involved was determined by EPMA. A concentration profile measured from a specimen annealed at 375 °C for 672 h is shown in Fig. 5. The average composition of the Zn-rich solid solution (about 0.9 wt% Al) as well as the overall composition of the (decomposed upon cooling, cf.

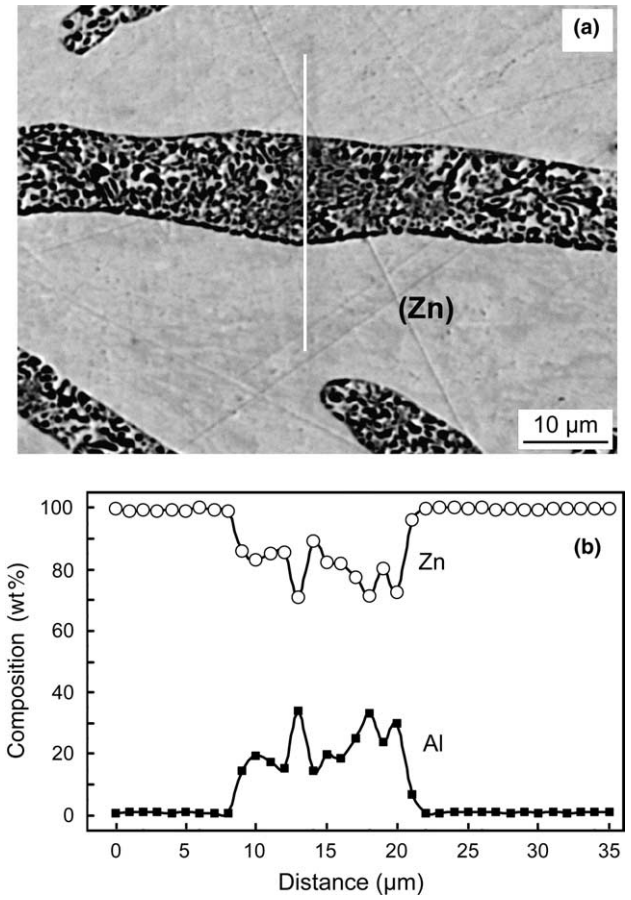

Fig. 5. Secondary-electron micrograph of a specimen annealed at 375 °C for 672 h (a). Composition profile along the line indicated in the micrograph as determined by EPMA (b).

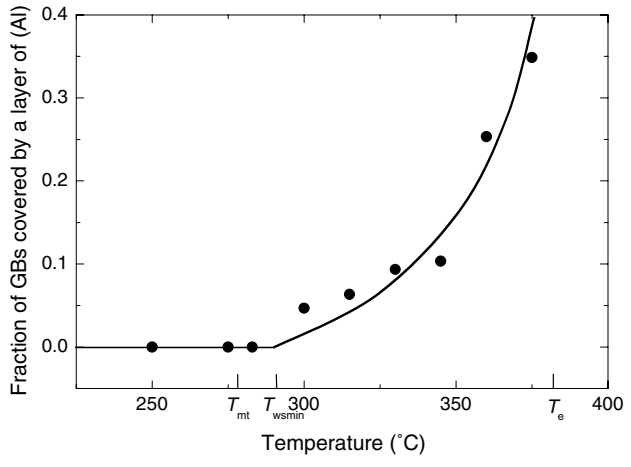

Fig. 6. Temperature dependence of the fraction of Zn-rich phase/Zn-rich phase GBs fully wetted by a continuous layer of the Al-rich phase. The temperatures T_{mt} and T_e of the bulk monotectoid and eutectic transformations have been indicated. T_{wsmin} is the minimal temperature of GB wetting by a solid phase. The data points for every temperature are averages of the data given in Table 1 for the different annealing times at each temperature.

Section 3.1) Al-rich solid solution (about 21 wt% Al) correspond well with the equilibrium values for these phases at a temperature slightly higher than T_{mt} (Fig. 2), thereby supporting the discussion in Section 3.2. The fine microstructure due to the monotectoid decomposition of the Al-rich phase upon cooling is observed in Fig. 5(a) and is revealed by oscillations in the concentration profile. XRD patterns from samples annealed at 375 °C for 672 and 2016 h were acquired. The calculated lattice parameters from the fitted XRD patterns are close to those reported in the literature for pure Al and for pure Zn. These results are consistent with the results from the metallographic observations and from the EPMA measurements, recognizing the decomposition of the Al-rich phase by monotectoid decomposition upon cooling after the anneal.

3.4. Quantification of the solid-phase wetting

The fraction of GBs fully covered by continuous layers of the Al-rich solid solution has been determined at each annealing temperature. A total of about 100 GBs was considered. The data obtained at the applied temperatures and annealing times have been gathered in Table 1. Evidently, the fraction of wetted GBs does *not* depend on annealing time at constant temperature. The temperature dependence of the fraction of GBs covered by a continuous layer of the Al-rich phase is shown in Fig. 6. The temperatures of the bulk monotectoid and eutectic transformations, T_{mt} and T_e, have been indicated. Below T_{mt} no GB was covered by a continuous layer of a solid phase (Fig. 4(a)). At $T = 283$ °C ($>T_{mt}$) all GBs contain only chains of isolated Al-rich phase particles (Fig. 4(d)). At 300 °C the first GBs occur which are completely covered by a continuous layer of the Al-rich phase. Hence, the minimal temperature of GB wetting by a solid phase, T_{wsmin}, for Zn-rich phase/Zn-rich phase GBs is in the range 283–300 °C. The corresponding tie-line has been drawn in the phase diagram (Fig. 2). The fraction of covered GBs increases with increasing temperature. The fraction of covered GBs does not reach 100%. Just below the eutectic tempera-

Table 1
Fraction of Zn-rich phase/Zn-rich phase GBs wetted by the Al-rich phase.

T (°C)	$t = 336$ h	$t = 672$ h	$t = 2016$ h
250	0	0	0
275	0	0	0
283	0	0	0
300	0.05	0.05	0.04
315	0.06	0.06	0.07
330	0.09	0.09	0.10
345	0.12	0.09	0.11
360	0.25	0.25	0.26
375	0.36	0.35	0.34

ture, T_e, the fraction of covered GBs equals only about 35%. This implies that T_{wsmax} (see Section 2) is higher than T_e and no T_{wsmax} tie-line of complete solid-phase wetting can be indicated.

The increase in the fraction of wetted GBs with increasing temperature is indicative of the presence of GBs in the specimens with different grain-boundary energies. Even for a single GB, the GB energy is not constant: differently oriented parts of a curved GB have different energies [21,22]. Thus, GBs could be found where parts with different orientations can be either completely (section AB in Fig. 7(a)) or incompletely (section BC in Fig. 7(a)) covered by the second solid phase.

The minimal value for the GB energy of a high-angle GB occurs for a twin GB. Therefore, twin GBs must have the highest possible critical temperature, T_{ws}. Twin plates in the Zn-rich phase (matrix) grains were recognized easily in the studied specimens using optical microscopy by applying polarized light. Indeed, even at the highest temperature studied (375 °C) twin GBs were never covered with a continuous layer of the Al-rich phase (Fig. 7(b)). Furthermore, the contact angle θ at the intersection of the precipitate particle and the twin GB is close to 180° (Fig. 7(b)). Further, note that the Al-rich phase particles on the twin GB are not even elongated along the twin GB. For chains of particles on other GBs the value of θ is between 30° and 100°. Evidently, T_{ws} correlates with the GB energy: the lower $\sigma^{\alpha\alpha}_{GB}$, the higher T_{ws}. For the case of *liquid* wetting it has also been shown that GB character/energy correlates with occurrence of wetting [23].

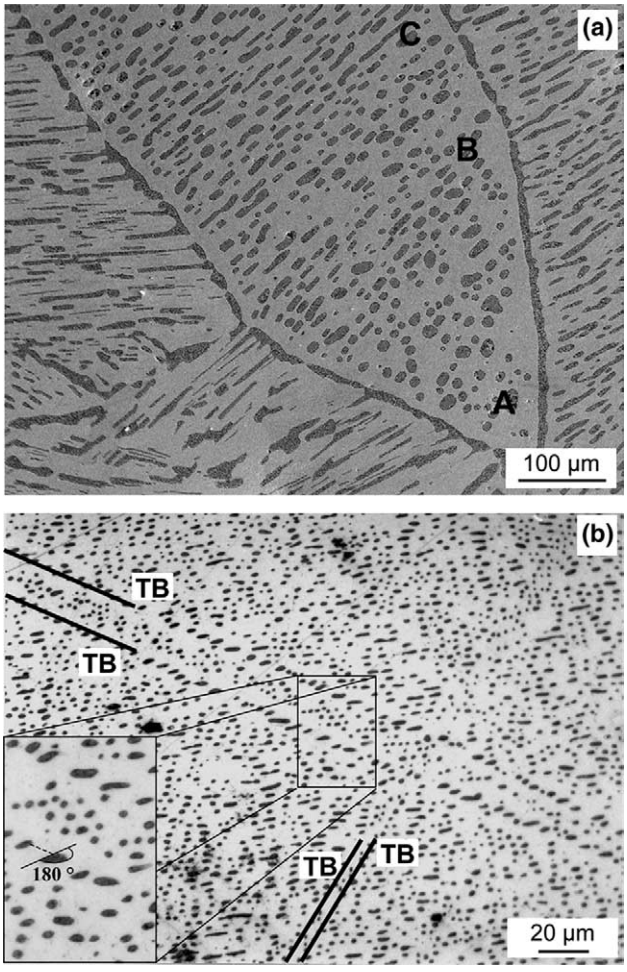

Fig. 7. (a) Curved Zn-rich phase/Zn-rich phase GB in a specimen annealed at 375 °C for 672 h (optical micrograph). Due to the inclination dependence of GB energy, the section AB with (apparently) relatively high $\sigma^{\alpha\alpha}_{GB}$ is wetted by a continuous layer of the Al-rich phase, and the section BC with (apparently) relatively low $\sigma^{\alpha\alpha}_{GB}$ is occupied by a chain of Al-rich phase particles. (b) Twin GBs in the Zn-rich phase of a specimen annealed at 375 °C for 336 h (optical micrograph). Due to the low GB energy of twin GBs, the twin boundaries GBs are not wetted but are occupied by chains of Al-rich phase particles. TB, twin boundary.

3.5. Growth kinetics of the Al-rich phase formed at the GBs

The increase of the (average) thickness, L, of the Al-rich phase formed at the GBs was measured. Either chains of elongated lens-like precipitates ($T < T_w$) or layers ($T > T_w$) occur. In both cases L was determined as the average of 40–50 measurements. A parabolic growth for L was observed with increasing annealing time, t (e.g. see Fig. 8(a)). The kinetic growth parameter $k = L^2/t$, as determined from least-squares fitting of straight lines to the data in plots of L^2 vs. t for the temperatures investigated, increases exponentially with increasing temperature (i.e. Arrhenius behaviour occurs; see Fig. 8(b)). It follows that the kinetics of thickness growth of both the (isolated) elongated precipitates and the layers can be described by one and the same Arrhenius plot, implying that the corresponding thickness increases are controlled by the same mechanism.

The results shown in Fig. 8 indicate that the growth is controlled by a diffusion process: the activation energy, Q, was determined as 96 kJ/mol and the pre-exponential factor, k_0, was found to be about 4×10^{-9} m^2/s. For comparison, the Arrhenius plots for the self-diffusion coefficients, D, of Zn [24,25] are also shown in Fig. 8(b) (diffusion data on Al bulk diffusion in Zn are not available in the literature). The value of Q for (lateral) growth of the Al-rich phase at the GBs agrees very well with the Q values for bulk self-diffusion for the diffusion perpendicular and parallel to the crystal c-axis in Zn, (96 and 92 kJ/mol, respectively [25]). It is concluded that the thickness increase of the Al-rich phase formed at the GBs is controlled by volume diffusion in the Zn-rich phase.

4. Final remark

An important difference between GB wetting by a liquid phase and GB wetting by a solid phase can be

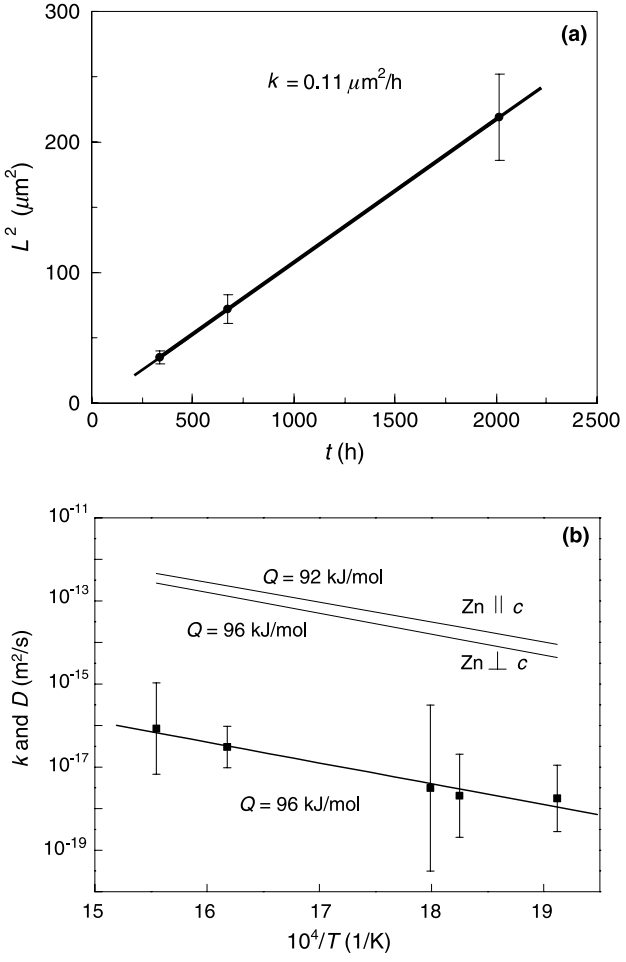

Fig. 8. (a) Parabolic growth of the thickness L of Al-rich phase formed at the GBs in specimens annealed at 345 °C. (b) Arrhenius plot of the kinetic growth constant k. The data for the bulk self-diffusion coefficients of Zn perpendicular and parallel to the crystal c-axis (thin lines: [24,25]) are shown for comparison. The variation of the k values as indicated in (b) follows from the possible variations in k as determined from least-squares fittings as that shown in (a).

indicated. In general in a two-phase ($\alpha + \beta$) region of a (binary) phase diagram α/α, β/β and α/β interfaces can occur. The composition of the binary Zn–Al alloy of this study was such that in the two-phase region analysed (see Fig. 2) β/β (i.e. Al-rich phase/Al-rich phase) GBs were practically not observed (see Section 3.1). Now consider an alloy of composition involving that a relatively large amount of β-phase occurs in the ($\alpha + \beta$) phase region. Then a relatively large amount of β/β GBs can be present. The β/β GBs can in principle also exhibit wetting: wetting by a solid α-phase. Generally, $T_{ws\beta\beta}$ will not be the same as $T_{ws\alpha\alpha}$. Hence, two kinds of GB wetting tie-lines can be drawn in the two-phase ($\alpha + \beta$) area of the phase diagram: one at $T_{ws\alpha\alpha}$ for wetting of α/α GBs by the β-phase and one at $T_{ws\beta\beta}$ for wetting of β/β GBs by the α-phase (Fig. 1(a)).

If $T_{ws\alpha\alpha} < T_{ws\beta\beta}$, upon increasing the temperature α/α GBs will be first wetted by the β-phase and when the temperature is higher than $T_{ws\beta\beta}$, β/β GBs will be wetted by the α-phase. Eventually, at sufficiently high temperature, only α/β IBs are stable in the polycrystal. This must lead to a configuration of α and β based on the alternating principle as exhibited by the light and dark fields on a chess-board (Fig. 1(f)).

5. Conclusions

- The transition from incomplete coverage of Zn-rich phase/Zn-rich phase grain boundaries by an Al-rich solid phase to complete wetting of the grain boundary by a continuous Al-rich phase layer occurs upon increasing the temperature at a critical temperature of solid-state wetting, T_{ws}.
- The critical temperature T_{ws} is different for grain boundaries and grain-boundary areas with different energies: T_{ws} decreases for increasing grain-boundary energy.
- The tie-line for the minimal temperature of wetting by a solid phase, T_{wsmin}, was determined for the Zn-rich phase + Al-rich phase two-phase area of the Al–Zn phase diagram confined by the monotectoid temperature, T_{mt}, and by the eutectic temperature, T_e. T_{wsmin} in the Zn–Al system lies slightly above T_{mt}.
- T_{wsmax} in the Zn–Al system lies above the temperature of the eutectic transformation, T_e.
- The fraction of grain boundaries wetted by a solid phase depends only on the temperature and not on the annealing time, and increases from 0% to about 35% with increase of temperature from T_{wsmin} to T_e.
- The thickness of the Al-rich phase formed at the grain boundaries is controlled by volume diffusion in the Zn-rich phase.

Acknowledgements

This investigation was partly supported by the German Research Foundation (DFG), NATO Linkage Grant (Contract PST.CLG.979375), the German Federal Ministry of Education and Research (BMBF), INTAS (Contract 03-51-3779), and the Russian Foundation for Basic Research (Contract 04-03-32800).

References

[1] Christian JW. The theory of transformations in metals and alloys, part I. 2nd ed. Oxford: Pergamon Press; 1975. p. 452.
[2] Herring C. Surface tension as a motivation for sintering. In: Kingston WE, editor. The physics of powder metallurgy. New York: McGraw–Hill; 1951. p. 143.
[3] Novikov II. Theory of thermal treatment of metals. 4th ed. Moscow: Metallurgia; 1986. p. 480 [in Russian].
[4] Schumann H. Metallography. 13th ed. Leipzig: Deutscher Verlag für Grundstoffindustrie; 1991 [in German].

[5] Geguzin YE. Physics of sintering. 2nd ed. Moscow: Nauka; 1984. p. 280 [in Russian].
[6] Eremenko VN, Naidich YV, Lavrinenko IA. Sintering in the presence of liquid phase. Kiev: Naukova Dumka; 1968. p. 132 [in Russian].
[7] Skorokhod VV, Panichkina VV, Prokushev NK. Poroshk Metall 1986;8:14 [in Russian].
[8] Huppmann WJ, Riegger H. Acta Metall 1975;23:965.
[9] Iribarren MJ, Agüero OE, Dyment F. Defect Diff Forum 2001;194–199:1211.
[10] Apykhtina I, Bokstein B, Khusnutdinova A, Peteline A, Rakov S. Defect Diff Forum 2001;194–199:1331.
[11] Eustathopoulos N, Coudurier L, Joud JC, Desre P. J Crystal Growth 1976;33:105.
[12] Rabkin EI, Semenov VN, Shvindlerman LS, Straumal BB. Acta Metall Mater 1991;39:627.
[13] Rabkin E, Weygand D, Straumal B, Semenov V, Gust W, Brechet Y. Philos Mag Lett 1996;73:187.
[14] Straumal B, Muschik T, Gust W, Predel B. Acta Metall Mater 1992;40:939.
[15] Straumal B, Molodov D, Gust W. J Phase Equilibr 1994;15: 386.
[16] Straumal B, Rabkin E, Lojkowski W, Gust W, Shvindlerman LS. Acta Mater 1997;45:1931.
[17] Straumal BB, López GA, Mittemeijer EJ, Gust W, Zhilyaev AP. Defect Diff Forum 2003;216–217:307.
[18] López GA, Straumal BB, Gust W, Mittemeijer EJ. In: Zehetbauer MJ, Valiev RZ, editors. Nanomaterials by severe plastic deformation. Fundamentals – processing – applications. Weinheim: Wiley–VHC; 2004. p. 642.
[19] Massalski TB et al., editors. Binary alloy phase diagrams. Materials Park, OH: ASM International; 1993. p. 239.
[20] Puchou JL, Pichoir E. La Res Aerospatiale 1984;3:13.
[21] Muschik T, Laub W, Finnis MW, Gust W. Z Metallkd 1993;84:596.
[22] Barg AI, Rabkin E, Gust W. Acta Metall Mater 1995;43:4067.
[23] Wynblatt P, Takashima M. Interface Sci 2001;9:265.
[24] Peterson NL, Rothman SJ. Phys Rev 1967;163:645.
[25] Mehrer H, editor. Landolt–Börnstein, vol. 26, Diffusion in solid metals and alloys. Berlin: Springer, 1990. p. 192.